수의학석사학위논문

소 프리온 단백질 유전자 과발현 형질전환 마우스를 이용한 소해면상뇌증 지속감염 세포의 생물학적 및 생화학적 특성 분석

Biological and Biochemical Characterization of M2B Cells in Transgenic Mice Overexpressing Bovine Prion Protein

2017년 8월

서울대학교 대학원

수의학과 수의병리학 전공

서 태 영

Abstract

Biological and Biochemical Characterization of M2B Cells in Transgenic Mice Overexpressing Bovine Prion Protein

Tae-Young Suh
Department of Veterinary Medicine
The Graduate School
Seoul National University

M2B cells with persistent classical bovine spongiform encephalopathy (C-BSE) have been established previously. In this study, we performed strain characterization of the M2B cell line in bovine PrP^{C} overexpressing mice (Tg 1896). Mice intracranially inoculated with M2B cells and C-BSE survived for 451 ± 7 and 465 ± 31 days post inoculation, respectively. Although biochemical properties, including deglycosylation and conformational stability, differed between M2B cells and C-BSE, inoculation with M2B cell lysates and C-BSE resulted in comparable phenotypes. Comparable vacuolation scores and PrP^{Sc} depositions were observed in the brain

of Tg 1896 inoculated with both M2B cell lysates and C-BSE. Our results show that biochemical and biological characteristics of M2B cells and C-BSE are classifiable in the same strain.

Keywords : BSE, prion, M2B cell line, persistent C-BSE cell line, strain characterization, mouse bioassay

Student Number : 2015-21817

Contents

List of Abbreviations

APHA	Animal and Plant Health Agency
APQA	Animal and Plant Quarantine Agency
BSE	Bovine spongiform encephalopathy
C−BSE	Classical type of bovine spongiform encephalopathy
DPI	Days post inoculation
GdnHCl	Guanidine hydrochloride solution
GPI	Glycosyl−phosphatidylinositol
H−BSE	Atypical H−type bovine spongiform encephalopathy
L−BSE	Atypical L−type bovine spongiform encephalopathy
MDBK cell	Madin−Darby Bovine Kidney
M2B cell	Cell line with persistent C−BSE
PK	Proteinase K
PRNP	Prion protein
PrP^{C}	Normal host prion protein
PrP^{Sc}	Abnormal, disease−associated form of prion protein
Tg M2B	Transgenic bovine mice inoculated with M2B cell lysates
Tg C−BSE	Transgenic bovine mice inoculated with homogenates of brains with C−BSE
TSEs	Transmissible spongiform encephalopathies

List of Table

List of Figures

Introduction

Transmissible spongiform encephalopathies (TSEs) are fatal infectious neurodegenerative diseases affecting human and animals. TSEs include variant and sporadic Creutzfeldt-Jakob disease in human, scrapie in sheep and goats, chronic wasting disease in deer, transmissible mink encephalopathy in mink and bovine spongiform encephalopathy in cattle. Bovine spongiform encephalopathy (BSE) is one type of TSEs causing fatal infectious neurodegenerative diseases in cattle (Prusiner 2004). The origin of BSE has not been fully identified; however, meat and bone meals derived from cattle with BSE are regarded as a major route of BSE transmission. Moreover, the agent causing BSE may be identical to that causing variant Creutzfeldt-Jakob disease in humans (Will and Zeidler 1996; Chazot et al. 1996). The key phenotypic characteristic of prion disease is the conformational change from the normal host prion protein (PrP^{C}) to abnormal, disease-associated form of prion protein (PrP^{Sc}). While PrP^{Sc} shares the same amino acid sequence with PrP^{C}, PrP^{C} has high solubility in detergent, sensitivity in proteinase K, α-helix rich structures. In contrast, PrP^{Sc} has

insolubility in detergent, resistance in proteinase K, β-sheet rich structures (Fig. 1) (Caughey et al. 1991). The protease resistant core of PrP^{Sc} is considered infectious and unique properties.

TSEs strains can be defined on the basis of differences in the conformation, glycosylation ratio, protease resistance, and aggregation state of the core of PrP^{Sc} (Bruce and Fraser 1991; Caughey et al. 1991; Meier et al. 2003; Xanthopoulos et al. 2009; Stahl et al. 1993; Butler et al. 1988). PrP^{C} and PrP^{Sc} consist of 208-220 amino acid residues depending on species, and contain two N-linked glycosylation site, disulfide bridge and C-terminal glycosyl-phosphatidylinositol (GPI) membrane anchor (Fig. 2) (Wopfner et al. 1999; Gill et al. 2000). The N-linked glycosylation site represents 3 types of glycosylation form which consist of un-, mono-, diglycosylated depending on attaching the number of glycans (Rudd et al. 1999). In hydrophobic regions, caveolae-like domains existed, and was suggested playing a key role in PrP^{C} converted into PrP^{Sc} (Vey et al. 1996). In addition, mice inoculated with TSEs can serve as strain characterization and provide reliable indicators for incubation periods and vacuolar degenerative patterns,

referred to as lesion profiles (Fraser et al. 1992; Fraser and Dickinson 1968; Green et al. 2005). Recently, rare atypical forms of BSE have been reported as active surveillance progressed (Buschmann et al. 2006; Biacabe et al. 2004; Casalone et al. 2004). These atypical forms were divided in accordance with western blot analysis of PrP^{Sc} profiles. One of these atypical forms showed lower molecular size (L-BSE) and the other one showed higher molecular size (H-BSE) when compared to the classical type of BSE (C-BSE) (Biacabe et al. 2004; Casalone et al. 2004). Both, molecular and biochemical properties, including incubation periods, PrP^{Sc} profiles, and histopathology, support that L-BSE and H-BSE were differentiated from C-BSE (Baron et al. 2006). Conceivably, different TSEs strains exhibit different biological and pathological profiles in the central nervous systems.

The mouse bioassay is the gold standard to identify biological properties of TSEs strains. However, there are major disadvantages to this method, such as the long incubation periods required (at least several months even in transgenic mice overexpressing Bovine PRNP) and the number of animals sacrificed

(Fraser and Dickinson 1968; Dickinson, Meikle, and Fraser 1968; Castilla et al. 2003). Therefore, considerable effort has been focused on replacing the animal experimental model with an *in vitro* assay using cell lines susceptible to BSE. Unfortunately, the number of studies investigating cell line with persistent TSE is limited. Rather, mouse-derived models (including a microglial cell line established from PrP^{C} overexpressing mice, peripheral neuroglial cell line, and murine neuroblastoma cell line) have been intensely investigated (Archer et al. 2004; Iwamaru et al. 2007; Butler et al. 1988). Previously, a cell line with persistent C-BSE (M2B cells) has been established using Madin-Darby Bovine Kidney (MDBK) cells overexpressing bovine cellular prion protein through a lentiviral expression system (Tark et al. 2015). However, biochemical properties of the M2B cell line, including the glycoform ratio and molecular weight of deglycosylated PrP^{Sc}, were different from biochemical properties of C-BSE. In order to utilize M2B cells in prion studies, it is necessary to confirm that the PrP^{Sc} in M2B cells originates from C-BSE.

We hypothesized that PrP^{Sc} in M2B was identical to that in

BSE. To address this question, we compared histopathological findings in mouse brains inoculated with M2B cell lysates and homogenates of cattle brain with C-BSE. Furthermore, we present biochemical properties of PrP^{Sc} of M2B cells by comparing glycoform ratio, deglycosylaiton, and conformational stability of PrP^{Sc}. On the basis of these criteria, we verified that M2B cells had persistent C-BSE, and then it contributes to using M2B cells for therapeutic development, a study on pathogenesis and metabolic interaction.

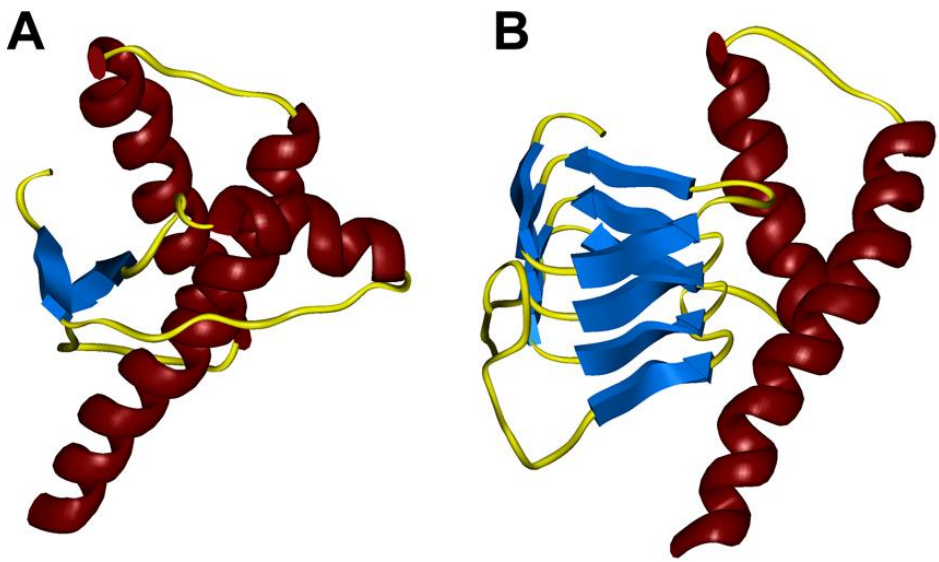

Figure 1. 3-dimentional structures PrP^{C} and PrP^{Sc}

PrP^{C} (A) is composed of mostly alpha-helical structures (red spiral shape) and less beta-sheet structures (blue arrow). But the increase of beta-sheet structures is observed in PrP^{Sc} (B). Mostly, the 90-160 amino acid regions are altered beta-sheet structures, while the C-terminal is preserved original structure (Caughey et al. 1991).

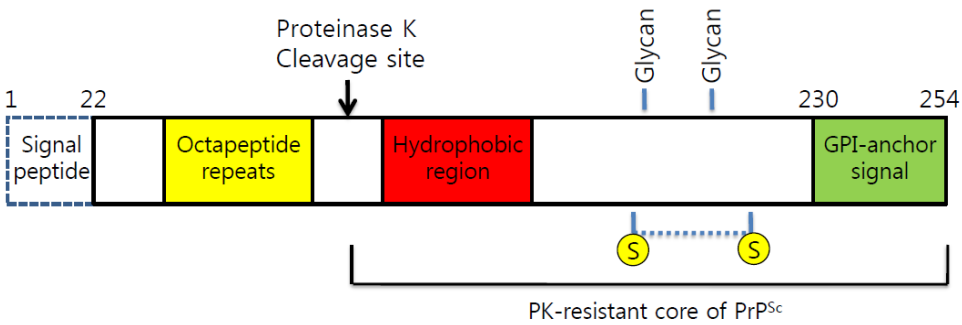

Figure 2. Schematic diagram of mammal PRNP

The undigested PrP has 254 amino acid residues including N-terminal signal peptide, metal ion-binding octapeptide repeats, di-sulfide bridge, N-linked glycosylation sites (Glycan), GPI-anchor attached signal and caveolae-like domain contained hydrophobic region (Gill et al. 2000).

Materials and Methods

Inocula preparation

An M2B cell line with persistent C-BSE has been established in a previous study (Tark et al. 2015). MDBK cell line (C1-2F) overexpressing bovine PRNP gene at an advance stage of persistent infection, was prepared as a negative control. M2B cells were cultured in a biosafety level III laboratory (Permission Number : KCDC-16-3-03). The cells were grown in completed medium [Dublecco s modified Eagle s medium/F12 supplemented with 10% fetal bovine serum, 100× antibiotics (penicillin and streptomycin), non-essential amino acid, L-glutamine]. Inocula were prepared from the M2B cell lysates at 35th passage in saline (3×10^7 cells/ml). As a positive control, 10% (w/v) cattle brain homogenates with C-BSE (APHA, UK) were prepared in normal saline. MDBK C1-2F cell lysates (3×10^7 cells/ml) and 10% (w/v) normal cattle brain homogenates in saline were prepared as negative controls. Cell lysates were homogenized by freezing and thawing three times.

Mouse inoculation and sampling

Transgenic Tg 1896 mice overexpressing bovine PRNP gene were obtained from the Animal and Plant Health Agency (APHA), and were kept under specific-pathogen-free (SPF) conditions during the experiments. Before injection, the genetic background of all transgenic mice was assessed by polymerase chain reaction using bovine PRNP primers. Eight-week-old mice were anaesthetized with isoflurane/O_2 and inoculated intracranially with 20 μl of the each inoculum. Ten mice were inoculated with M2B cell lysates. For positive and negative controls, 4 mice were inoculated respectively. Inoculated mice were housed in isolators placed in the animal care facility of the biosafety level III laboratory. Health status and clinical signs were observed daily. Clinical signs included rough hair coat, sticky eyes, emaciation, hunched back, limb paresis, convulsion, and depression (Dickinson, Meikle, and Fraser 1968). When a mouse showed more than three of these symptoms over one week, euthanasia and necropsy were performed. One half of each brain was fixed in 10% neutral buffered formalin for

histopathology and the other half was homogenized at 10% (w/v) concentration in normal saline for biochemical assays. Survival times were defined as the number of days from inoculation to the terminal stage of the disease. All animal experiments were approved according to the guideline of APQA Animal Ethics Committee (Approval number : 2016-449). Statistical analysis was performed using the GraphPad-Prism software.

Western blotting

Brain homogenates prepared in saline were mixed with 15 μl of PrP^{Sc} lysis buffer, composed of PBS containing 0.5% TritonX-100, 5 mM EDTA, 150 mM NaCl, 0.05% Digitonin (Sigma-Aldrich) and complete mini protease inhibitors (Roche Applied Science). The samples were mixed with 5 μl collagenase (20 mg/ml) and 8 μl of DNase I (10 mg/ml) and incubated for 1 h at 37℃. To digest PrP^{C}, 8 μl of PK (1 mg/ml) was added and incubated at 37℃ for 1 h. The digested samples were mixed with 8 μl of pefabloc and centrifuged at 20,000 g for 15 min. After discarding the supernatant, 20 μl of 4% sodium dodecyl sulfate (SDS) was added. Samples were boiled at

100℃ for 5 min, and 400 μl of pre-cooled methanol were added. Samples precipitated overnight at −20℃. After precipitation, dried pellets were collected after 10 min of centrifugation at 20,000 g. Dried pellets were boiled at 100℃ for 5 min in 20 μl of SDS sample buffer and separated by electrophoresis at 100 V for 90 min in NuPAGE 12% Bis-Tris gel. Proteins were transferred onto PVDF membranes (Immonilon P, Merk Millipore) in transfer buffer at 400 mA for 90 min. Membranes were blocked with 0.02% I-Block (Tropix) in tris-buffered saline (TBS) for 30 min and rabbit anti-PrP polyclonal antibody S1 was applied (produced by the APQA). Immunoreactive bands were developed with CDP STAR (Applied Biosystems) and analyzed using an LAS 4000 chemiluminescence system (Fuji). Prior to the analysis, PrP^{Sc} quantities were equalized by serial loading volumes. Glycoform profiles (i.e., ratio of diglycosylated, monoglycosylated and unglycosylated PrP^{Sc}) were analyzed by ImageQurantTL 1D gel analysis (Fuji).

Deglycosylation of PrP^{Sc}

In order to remove N-linked glycosylation, PNGase F (New

England BioLabs) was used. 5 μl of brain homogenate were mixed with 15 μl of PrP^{Sc} lysis buffer and 4 μl of PK (1 mg/ml) and incubated at 37℃ for 1 h. The incubated samples were centrifuged at 20,000 g for 1 h and 8 μl of 30% sarkosyl was added. After discarding the supernatant, samples were dissolved in 10 μl of glycoprotein denaturation buffer and heated at 100℃ for 10 min. After cooling heated samples, 2 μl of 10% NP40, 2 μl of 10× GlycoBuffer, 2 μl of PNGase and 4 μl of distilled water were added. The samples were incubated overnight at 37℃. Subsequently, samples were incubated with 20 μl of SDS sample buffer at 100℃ for 5 min. Samples were separated and blotted following a previously described western blotting method.

Conformational stability

Five microliters of a brain homogenate were mixed with 15 μl of PrP^{Sc} lysis buffer and 1 μl of PK (10 mg/ml) and incubated at 37℃ for 1 h. Guanidine hydrochloride solution (GdnHCl) at concentrations ranging from 0 to 4 M (final concentration) were added and incubated at 20℃ for 1 h while shaking gently.

Subsequently, samples were centrifuged at 20,000 g for 1 h and 8 μl of 30% sarkosyl were added. After discarding the supernatant, 20 μl of 4% SDS were added. Samples were boiled at 100℃ for 5 min, 400 μl of pre-cooled methanol were added, and samples were allowed to precipitate overnight at −20℃. After precipitation, dried pellets were collected by centrifugation at 20,000 g for 10 min. Dried pellets were boiled at 100℃ for 5 min in 20 μl SDS sample buffer. Samples were separated and blotted according to previously described western blotting methods. Statistical analysis was performed using the GraphPad-Prism software.

Histopathology

Mouse brains were fixed in 10% neutral buffered formalin and immersed in 88% formic acid for 1 h to inactivate PrP^{Sc}. After tissue processing and paraffin embedding, serial 5 μm thick sections were stained with H&E. The pattern of vacuolar changes was scored in 12 areas, namely the dorsal medullar nuclei (G1), cerebellar cortex (G2), superior colliculus (G3), hypothalamus (G4), central thalamus (G5), hippocampus (G6), septal nuclei (G7),

posterior cerebral cortex (G8), anterior cerebral cortex (G9), cerebellar white matter (W1), mesencephalic tegmentum (W2), and pyramidal tract (W3). The vacuolation score was established based on the pattern, size and density of the vacuoles using standard criteria (grade 0 for no and grade 5 for maximum vacuolation) (Fraser and Dickinson 1968).

Immunohistochemistry

Tissue sections were dewaxed, rehydrated with routine pretreatments including 30-min hydrated autoclaving at 121℃ in 500 ml of antigen-retrieval solution (DAKO). A polyclonal rabbit anti-PrP antibody (S1), biotinylated anti-rabbit secondary antibody, alkaline phosphatase-streptavidin conjugate, and 3-amino-9ethylcarbazole substrate were used for immunolabeling. Immunostaining was performed using a semi-automated immunostaining machine (BenchMark, Roche).

Result

Survival times and clinical signs in inoculated mice.

Attack rates and survival times of transgenic bovine mice inoculated with M2B cell lysates (Tg M2B) and homogenates of brains with C-BSE (Tg C-BSE) are shown in Table 1. Both Tg M2B and Tg C-BSE developed the disease during survival times and produced some common clinical signs, such as rough hair coat, sticky eye, and hunched back. Mice in the terminal stage showed convulsion, paralysis, and death. Survival times of Tg M2B and Tg C-BSE were 451 ± 7 days post inoculation (dpi) and 465 ± 31 dpi respectively. No significant difference in distributions of survival times between both groups was observed in an unpaired, two-tailed t-test ($p < 0.05$). Both groups showed 100% attack rates. No inoculum specific clinical signs were observed in this assay. Negative controls showed no clinical signs or death.

Table 1. Attack rate and survival times of mice inoculated with M2B cell lysates and C-BSE

Classification	Inocula	Attack Rate*	Survival times ±SEM (dpi)
Treatment	M2B cell lysates	10/10	451±7
Positive control	C-BSE	4/4	465±31
Negative control	C1-2F cell lysates	0/4	480**
	Normal bovine brain	0/4	480**

* Number of mice showed clinical signs / Number of mice inoculated

** Sacrificed

Pathological findings in inoculated mice

Lesion profiling of Tg M2B and Tg C-BSE was performed using hematoxylin and eosin staining (H&E). When using a semiquantitative method for lesion profiling, vacuolation scores of Tg M2B were comparable to those of Tg C-BSE (Fig. 3). Both groups showed moderate to severe vacuolar degeneration in dorsal medullar nuclei, central thalamus and septal nuclei. In addition, relatively severe vacuolar degeneration was observed in mesencephalic tegmentum compared with other white matter lesions (Fig. 4). Less than 10 vacuoles were observed in cerebellar cortex, superior colliculus, hypothalamus, hippocampus, posterior cerebral cortex, anterior cerebral cortex, cerebellar white matter, and pyramidal tract. The patterns of PrP^{Sc} depositions of Tg M2B were analogous to those of Tg C-BSE in immunohistochemistry (Fig. 5). Accumulation of PrP^{Sc} was observed multifocally in dorsal medullar nuclei, central thalamus and partially in posterior cerebral cortex, hippocampus and hypothalamus. Both Tg M2B and Tg C-BSE showed some multifocal plaque-like deposition of PrP^{Sc} in the central thalamus.

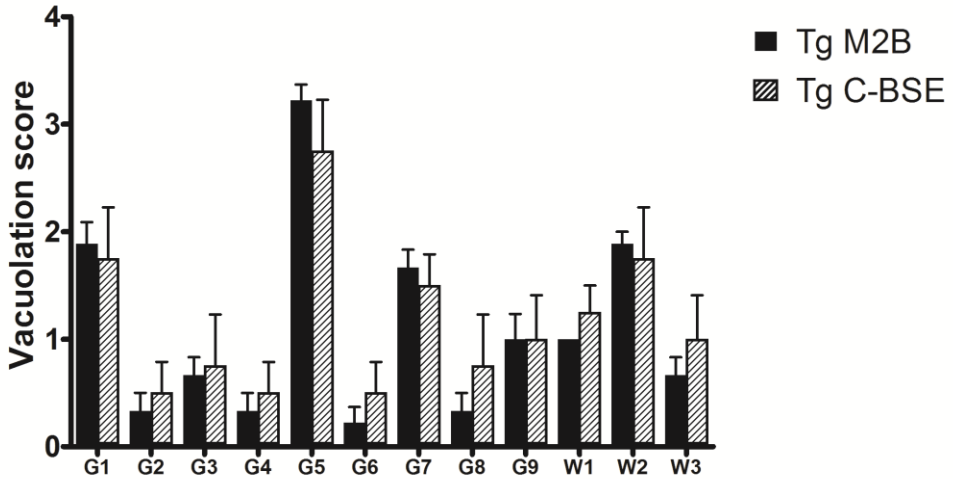

Figure 3. Neuropathological lesion profiles in Tg bovine mice

Vacuolar lesion profiles in Tg bovine mice brains infected with M2B cells (n = 10) or C-BSE (n = 4). Gray matter scoring: G1, dorsal medullar nuclei; G2, cerebellar cortex; G3, superior colliculus; G4, hypothalamus; G5, central thalamus; G6, hippocampus; G7, septal nuclei; G8, posterior cerebral cortex; G9, anterior cerebral cortex. White matter scoring: W1, cerebellar white matter; W2, mesencephalic tegmentum; W3, pyramidal tract. Blue circles represent the 10 mice inoculated with M2B cells; Red rectangles represent the 4 mice inoculated with C-BSE. Error bars, SEM.

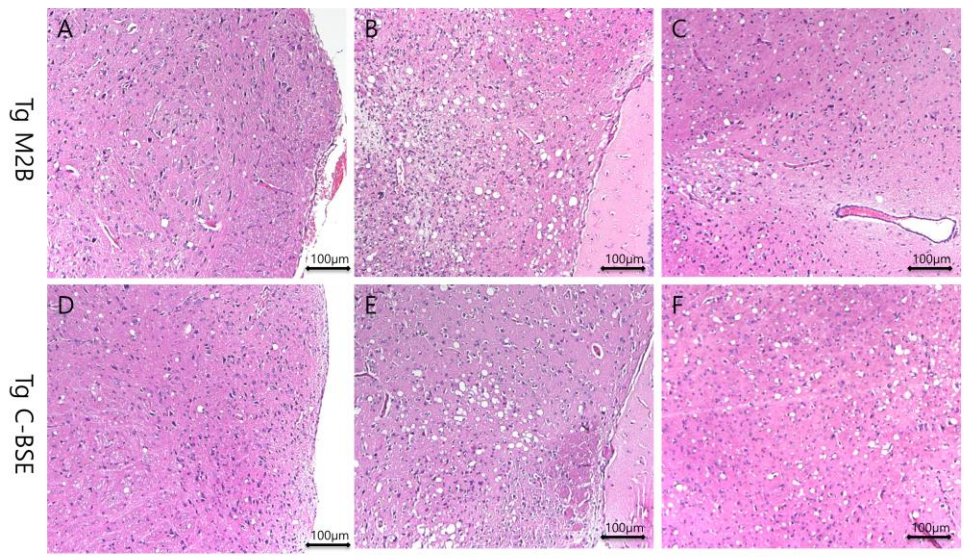

Figure 4. Hematoxylin and eosin staining of Tg M2B and Tg C-BSE

Vacuolation of the dorsal medullar nuclei in medulla sections of Tg M2B (A) and Tg C-BSE (D). Vacuolation of the thalamus in thalamic sections of Tg M2B (B) and Tg C-BSE (E), and mesencephalic tegmentum in midbrain section of Tg M2B (C), Tg C-BSE (F).

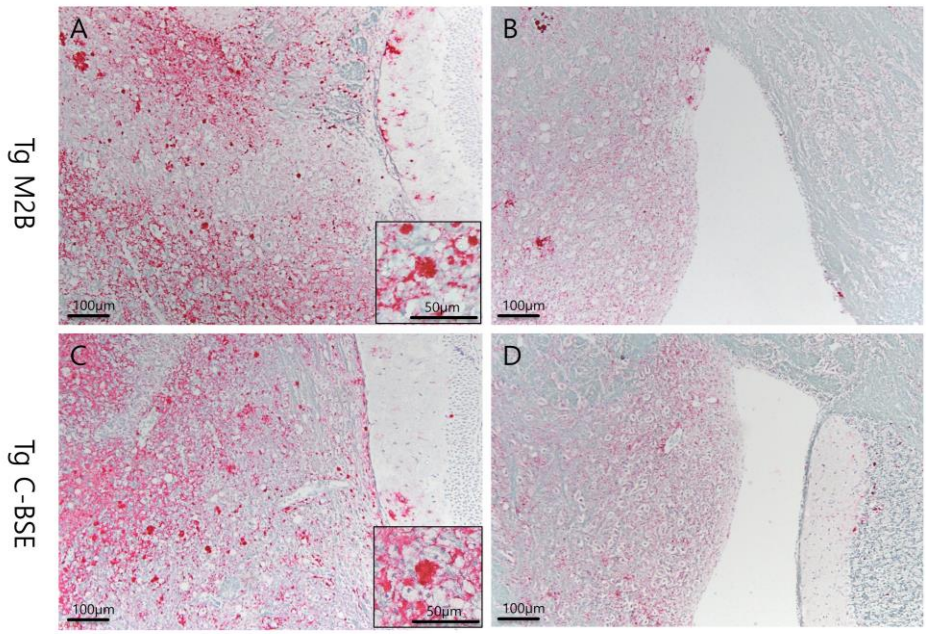

Figure 5. Immunohistochemistry of Tg M2B and Tg C-BSE using S1 antibody

PrP^{Sc} deposition in the central thalamus in thalamic sections of Tg M2B (A) and Tg C-BSE (C), small window: Plaque like depositions of PrP^{Sc}. PrP^{Sc} deposition in the dorsal medullar nuclei in medulla section of Tg M2B (B) and Tg C-BSE (D).

Biochemical properties of PrP^{Sc}

Biochemical properties of PrP^{Sc} (molecular weights and relative antibody immunoreactivity) in Tg M2B and Tg C-BSE were compared on the basis of immunoblotting and glycoform ratios. As shown in Fig. 6A, when samples were not treated with proteinase K (PK), both C-BSE and Tg C-BSE showed identical migration patterns. Tg M2B showed comparable patterns with C-BSE and Tg C-BSE; however, M2B cells showed different migration patterns both with and without PK treatment.

To compare PrP^{Sc} glycoform ratios in the different preparations, the relative immunoreactivity of diglycosylated, monoglycosylated, and unglycosylated PrP^{Sc} was analyzed. The relative immunoreactivity of Tg M2B and Tg C-BSE did not differ significantly at $p < 0.05$ (Fig. 6B). PrP^{Sc} glycoform ratios in both samples were similar to those of C-BSE, although the amount of unglycosylated PrP^{Sc} was lower in M2B cells than in the other samples.

To analyze the molecular weight of the PrP^{Sc} core, all samples were treated with PNGase F. In Tg C-BSE and Tg M2B

molecular weight of the PrP^{Sc} core was similar, although there was a slight change in the electrophoretic migration of deglycosylated PrP^{Sc} in M2B cells compared with that in C-BSE (Fig. 7). In addition, migration patterns of unglycosylated PrP^{Sc} from both Tg C-BSE and Tg M2B were similar to migration patterns of C-BSE than migration patterns of M2B cells. All PNGase F treated samples were completely deglycosylated and the susceptibility of PNGase F appeared negligible.

In the conformational stability assay, resistance to increasing concentrations of GdnHCl was determined. GdnHCl-induced unfolding of PrP^{Sc} was observed in the all samples (Fig. 8A); the percentage of PrP^{Sc} decreased as GdnHCl concentration increased. Relative conformational stability was compared on the basis of the GdnHCl concentration at which half of the PrP^{Sc} was denaturated ($GdnHCl_{1/2}$). M2B cells and C-BSE showed different denaturation curves and different $GdnHCl_{1/2}$ values, 1.38 ± 0.04 M and 1.90 ± 0.10 M, respectively. However, Tg M2B and Tg C-BSE showed similar conformational stability, as neither denaturation curves nor $GdnHCl_{1/2}$ values (2.31 ± 0.06 M and 2.37 ± 0.07 M, respectively) significantly differed at $p < 0.05$ (Fig. 8B).

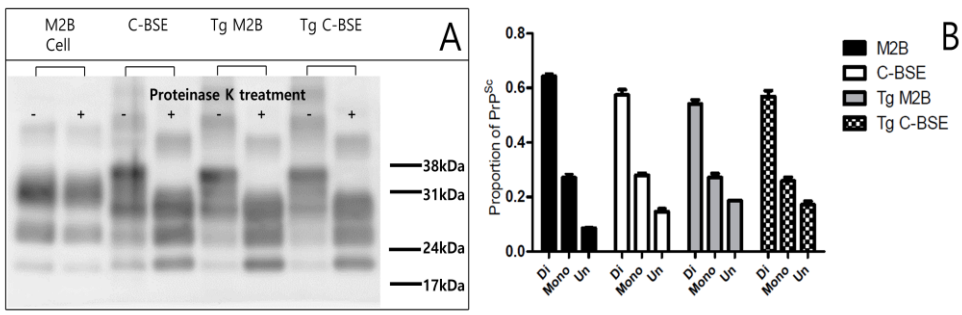

Figure 6. Western blot analysis and relative glycoform ratio of PrP^{Sc} in Tg M2B and Tg C-BSE

(A) C-BSE and mouse brain homogenates infected with C-BSE and M2B cells show different patterns before and after treatment with proteinase K. In contrast, M2B cells maintained the same pattern before and after digestion with proteinase K. (B) Relative proportion of PrP^{Sc} detected as diglycosylated (Di), monoglycosylated (Mono), unglycosylated (Un) PrP^{Sc}. Error bars, SEM.

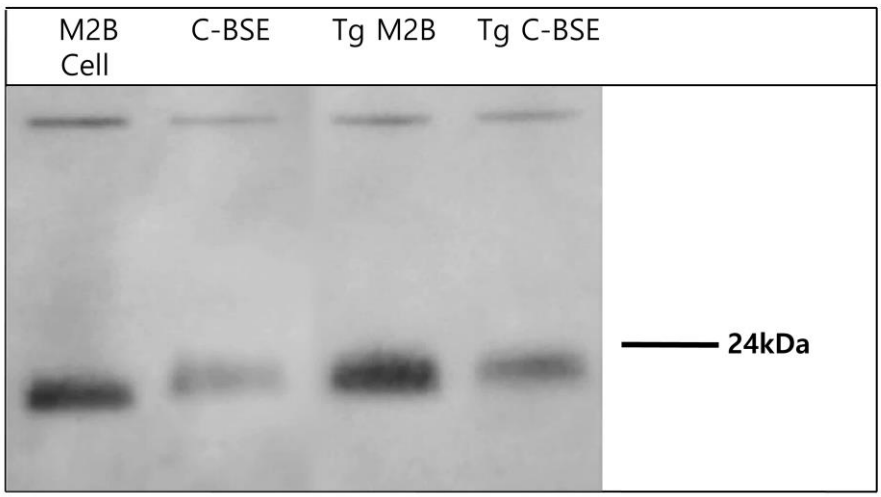

Figure 7. Deglycosylation of PrP^{Sc} in Tg M2B and Tg C-BSE

Molecular size of PrP^{Sc} from M2B cells was smaller than of PrP^{Sc} from C-BSE and homogenates of brain from Tg bovine mice infected with C-BSE. Molecular size of Tg M2B is similar to C-BSE than M2B cells.

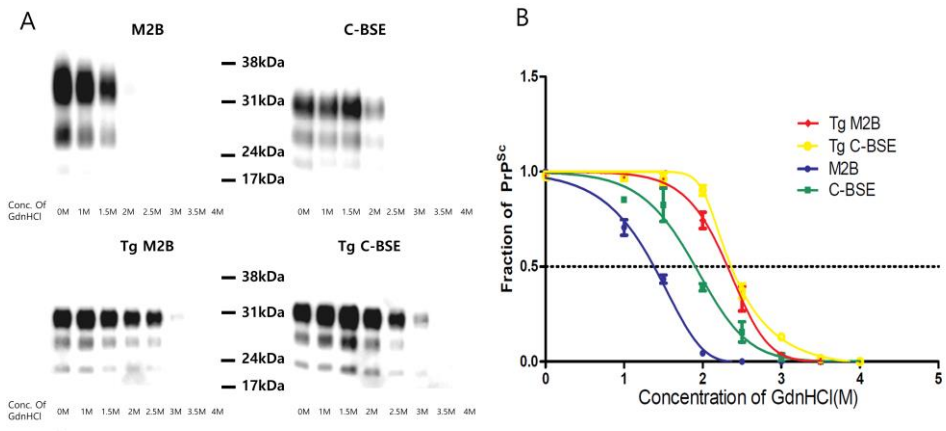

Figure 8. Conformational stability of PrP^{Sc} in Tg M2B and Tg C-BSE

(A) Western blotting of the samples. The amount of PrP^{Sc} was inversely proportional to the concentration of GdnHCl in all samples. (B) Fraction of PrP^{Sc} as a function of GdnHCl. PrP^{Sc} from M2B cells showed 1.38 ± 0.04 M at $GdnHCl_{1/2}$ and PrP^{Sc} from C-BSE showed 1.90 ± 0.10 M at $GdnHCl_{1/2}$. Conformational stability of PrP^{Sc} was comparable in Tg M2B and Tg C-BSE brain homogenates. $GdnHCl_{1/2}$ values were 2.31 ± 0.06 M and 2.37 ± 0.07 M, respectively. Error bars, SEM.

Discussion

M2B cells with persistent C-BSE have been established previously (Tark et al. 2015) and the M2B cell strain has been characterized in conventional VM/Dk mouse (unpublished). However, whether M2B cells and C-BSE induce the same neurodegenerative disease in cattle remained to be elucidated. Transgenic mouse models are useful tools to indirectly characterize the effect of M2B cells in cattle. Although the measurement of survival times is expensive and time-consuming, they are an important indicator for the disease: Survival times depend on PrP^{Sc} deposition lesions and neurodegenerative disease progress, which are caused by PrP^{Sc} inoculation (Fraser and Dickinson 1968). However, in primary passage, the same strain of PrP^{Sc} may result in different survival times (Bruce et al. 2002). To reduce influences on survival times because of the difference between inocula, we used semi-quantitative titration by enzyme-linked immunosorbent assay to equalize titer of PrP^{Sc}. The survival times of Tg M2B mice and Tg C-BSE were 451 ± 7 dpi and 465 ± 31 dpi, respectively (Table 1.). No significant difference was observed when comparing

survival times after M2B cell lysates and C-BSE inoculation.

Tg M2B and Tg C-BSE showed similar lesion profiles, consistent with previous reports on lesion profiles of Tg mice treated with C-BSE in the UK (APHA, unpublished data). In our study, both groups of inoculated mice showed higher scores for dorsal medullar nuclei, central thalamus, septal nuclei, and mesencephalic tegmentum than for other lesions (Fig. 5). Depositions of PrP^{Sc} detected by immunohistochemistry were consistent with lesion profiles. Taken together, these results indicate that the accumulation of PrP^{Sc} caused vacuolar degeneration. In addition, both Tg M2B and Tg C-BSE showed comparable multifocal plaque-like depositions in the central thalamus. Strain specific pathological properties of C-BSE were reproduced in M2B cells. However, different biochemical features were observed between C-BSE and M2B cells in biochemical analysis. First, immunoreactive bands of M2B cells were conserved after PK digestion, while immunoreactive bands of C-BSE were diminished after PK treatment. This possibly resulted from disturbed PK digestion due to some endogenous extracts in the M2B cell condition. This phenomenon has also been observed in

mouse neuroblastoma cells with persistent scrapie (Butler et al. 1988). In addition, other endogenous enzymes could have affected M2B cells before PK digestion. PK acts on the PK cleavage site (β−cleavage site) and after digestion of the C−terminal, the PK−resistant core of PrP^{Sc} remains (Prusiner et al. 1983). However, the other cleavage site (α−cleavage site) resides closer the C−terminal than the β−cleavage site. This digestion causes shorter residues of PrP^{Sc}. Several enzymes have generally been identified including ADAM family, plasmin and plasminogen (Liang and Kong 2012). These enzymes might be activated during cell culture or the cell lysis procedure.

Secondly, PrP^{C} appears in three different glycoforms, un−, mono− and diglycosylated form. Glycosylation happens in the endoplasmic reticulum by the attachment of glycan to the N−linked glycosylation site (Rudd et al. 1999). The three different glycoforms showed tissue−specific biochemical properties (Moudjou et al. 2001). Because the M2B cell line originated from the MDBK cell line (derived from kidney epithelium), it makes sense that the structure of prion proteins differs between brain tissue and M2B cells. Conclusively, these results were compatible

with previous reports that persistently infected cell lines preserved properties of PrP^{Sc} in serial passages (Arima et al. 2005).

Previous studies have shown that migration patterns of the PrP^{Sc} core fragment after digestion with PK represent strain specific properties (strain characterization) (Buschmann et al. 2006; Telling et al. 1996). However, recent studies have shown that biochemical properties such as glycoform profiles and molecular size of deglycosylated PrP^{Sc} were not conserved in persistently infected cells (Arima et al. 2005; Oelschlegel et al. 2015). Furthermore, murine GT1 cells persistently infected with different Creutzfeldt-Jakob disease agents showed identical PrP^{Sc} migration patterns (Arjona et al. 2004). Taken together, the conventional strain characterization method has certain limitations in persistently infected cells. Thus, a mouse bioassay was essential for strain characterization of M2B cells. Future studies should include *in vitro* bioassays of prion strain characterization to overcome limitation of mouse bioassays such as being time-consuming and posing ethical and financial problems.

Conclusion

In conclusion, the present study revealed biochemical and histopathological similarities of PrP^{Sc} obtained from M2B cells and C-BSE in transgenic mouse. The present data demonstrates the suitability of M2B cells as a tool to investigate prion diseases. However, it remains unclear why M2B cells, which showed different biochemical properties from C-BSE, induced the same pathological changes, and eventually recovered original properties. Further investigation of this phenomenon of a structural shift of PrP^{Sc} in cell cultures is necessary.

Reference

Archer, F., C. Bachelin, O. Andreoletti, N. Besnard, G. Perrot, C. Langevin, A. Le Dur, D. Vilette, A. Baron-Van Evercooren, J. L. Vilotte, and H. Laude. 2004. Cultured peripheral neuroglial cells are highly permissive to sheep prion infection, J Virol, 78: 482-90.

Arima, K., N. Nishida, S. Sakaguchi, K. Shigematsu, R. Atarashi, N. Yamaguchi, D. Yoshikawa, J. Yoon, K. Watanabe, N. Kobayashi, S. Mouillet-Richard, S. Lehmann, and S. Katamine. 2005. Biological and biochemical characteristics of prion strains conserved in persistently infected cell cultures, J Virol, 79: 7104-12.

Arjona, Alvaro, Laura Simarro, Florian Islinger, Noriyuki Nishida, and Laura Manuelidis. 2004. Two Creutzfeldt-Jakob disease agents reproduce prion protein-independent identities in cell cultures, Proc Natl Acad Sci U S A, 101: 8768-73.

Baron, T. G., A. G. Biacabe, A. Bencsik, and J. P. Langeveld. 2006. Transmission of new bovine prion to mice, Emerg Infect Dis, 12: 1125-8.

Biacabe, A. G., J. L. Laplanche, S. Ryder, and T. Baron. 2004. Distinct molecular phenotypes in bovine prion diseases, EMBO Rep, 5: 110-5.

Bruce, M. E., A. Boyle, S. Cousens, I. McConnell, J. Foster, W. Goldmann, and H. Fraser. 2002. Strain characterization of natural sheep scrapie and comparison with BSE, J Gen Virol, 83: 695-704.

Bruce, M. E., and H. Fraser. 1991. Scrapie strain variation and its implications, Curr Top Microbiol Immunol, 172: 125-38.

Buschmann, A., A. Gretzschel, A. G. Biacabe, K. Schiebel, C. Corona, C. Hoffmann, M. Eiden, T. Baron, C. Casalone, and M. H. Groschup. 2006. Atypical BSE in Germany-proof of transmissibility and biochemical characterization, Vet Microbiol, 117: 103-16.

Butler, D. A., M. R. Scott, J. M. Bockman, D. R. Borchelt, A. Taraboulos, K. K. Hsiao, D. T. Kingsbury, and S. B. Prusiner. 1988. Scrapie-infected murine neuroblastoma cells produce protease-resistant prion proteins, J Virol, 62: 1558-64.

Casalone, C., G. Zanusso, P. Acutis, S. Ferrari, L. Capucci, F. Tagliavini, S. Monaco, and M. Caramelli. 2004. Identification of a second bovine amyloidotic spongiform encephalopathy: molecular similarities with sporadic Creutzfeldt-Jakob disease, Proc Natl Acad Sci U S A, 101: 3065-70.

Castilla, J., A. Gutierrez Adan, A. Brun, B. Pintado, M. A. Ramirez, B. Parra, D. Doyle, M. Rogers, F. J. Salguero, C. Sanchez, J. M. Sanchez-Vizcaino, and J. M. Torres. 2003. Early detection of PrP^{res} in BSE-infected bovine PrP transgenic mice, Arch Virol, 148: 677-91.

Caughey, B. W., A. Dong, K. S. Bhat, D. Ernst, S. F. Hayes, and W. S. Caughey. 1991. Secondary structure analysis of the scrapie-associated protein PrP 27-30 in water by infrared spectroscopy, Biochemistry, 30: 7672-80.

Chazot, G., E. Broussolle, Cl Lapras, T. Blattler, A. Aguzzi, and N. Kopp. 1996. New variant of Creutzfeldt-Jakob disease in a 26-year-old French man, Lancet, 347: 1181.

Dickinson, A. G., V. M. Meikle, and H. Fraser. 1968. Identification of a gene which controls the incubation period of some strains of scrapie agent in mice, J Comp Pathol, 78: 293-9.

Fraser, H., M. E. Bruce, A. Chree, I. McConnell, and G. A. Wells. 1992. Transmission of bovine spongiform encephalopathy and scrapie to mice, J Gen Virol, 73: 1891-7.

Fraser, H., and A. G. Dickinson. 1968. The sequential development of the brain lesion of scrapie in three strains of mice, J Comp Pathol, 78: 301-11.

Gill, Andrew C., Mark A. Ritchie, Lawrence G. Hunt, Sarah E. Steane, Kenneth G. Davies, Sharon P. Bocking, Alexandre G. O. Rhie, Alan D. Bennett, and James Hope. 2000. Post-translational hydroxylation at the N-terminus of the prion protein reveals presence of PPII structure in vivo, The EMBO Journal, 19: 5324-31.

Green, R., C. Horrocks, A. Wilkinson, S. A. Hawkins, and S. J. Ryder. 2005. Primary isolation of the bovine spongiform encephalopathy agent in mice: agent definition based on a review of 150 transmissions, J Comp Pathol, 132: 117-31.

Iwamaru, Y., T. Takenouchi, K. Ogihara, M. Hoshino, M. Takata, M. Imamura, Y. Tagawa, H. Hayashi-Kato, Y. Ushiki-Kaku, Y. Shimizu, H. Okada, M. Shinagawa, H. Kitani, and T. Yokoyama. 2007. Microglial cell line established from prion protein-overexpressing mice is susceptible to various murine prion strains, J Virol, 81: 1524-7.

Liang, Jingjing, and Qingzhong Kong. 2012. α-Cleavage of cellular prion protein, Prion, 6: 453-60.

Meier, P., N. Genoud, M. Prinz, M. Maissen, T. Rulicke, A. Zurbriggen, A. J. Raeber, and A. Aguzzi. 2003. Soluble dimeric prion protein binds PrP^{Sc} in vivo and antagonizes prion disease, Cell, 113: 49-60.

Moudjou, Mohammed, Yveline Frobert, Jacques Grassi, and Claude La Bonnardière. 2001. Cellular prion protein status in sheep: tissue-specific biochemical signatures, J Gen Virol, 82: 2017-24.

Oelschlegel, A. M., M. Geissen, M. Lenk, R. Riebe, M. Angermann, H. Schatzl, and M. H. Groschup. 2015. A bovine cell line that can be infected by natural sheep scrapie prions, PLoS One, 10: e0117154.

Prusiner, S. B., M. P. McKinley, K. A. Bowman, D. C. Bolton, P. E. Bendheim, D. F. Groth, and G. G. Glenner. 1983. Scrapie prions aggregate to form amyloid-like birefringent rods, Cell, 35: 349-58.

Prusiner, Stanley B. 2004. Prion Biology and Diseases, Cold Spring Harbor Lab. Press, pp 653-715.

Rudd, P. M., T. Endo, C. Colominas, D. Groth, S. F. Wheeler, D. J. Harvey, M. R. Wormald, H. Serban, S. B. Prusiner, A. Kobata, and R. A. Dwek. 1999. Glycosylation differences between the normal and pathogenic prion protein isoforms, Proc Natl Acad Sci U S A, 96: 13044-9.

Stahl, N., M. A. Baldwin, D. B. Teplow, L. Hood, B. W. Gibson, A. L. Burlingame, and S. B. Prusiner. 1993. Structural studies of the scrapie prion protein using mass spectrometry and amino acid sequencing, Biochemistry, 32: 1991-2002.

Tark, D., H. Kim, M. H. Neale, M. Kim, H. Sohn, Y. Lee, I. Cho, Y. Joo, and O. Windl. 2015. Generation of a persistently infected MDBK cell line with natural bovine spongiform encephalopathy, PLoS One, 10: e0115939.

Telling, G. C., P. Parchi, S. J. DeArmond, P. Cortelli, P. Montagna, R. Gabizon, J. Mastrianni, E. Lugaresi, P. Gambetti, and S. B. Prusiner. 1996. Evidence for the conformation of the pathologic isoform of the prion protein enciphering and propagating prion diversity, Science, 274: 2079-82.

Vey, M., S. Pilkuhn, H. Wille, R. Nixon, S. J. DeArmond, E. J. Smart, R. G. Anderson, A. Taraboulos, and S. B. Prusiner. 1996. Subcellular colocalization of the cellular and scrapie prion proteins in caveolae-like membranous domains, Proc Natl Acad Sci U S A, 93: 14945-9.

Will, R., and M. Zeidler. 1996. Diagnosing Creutzfeldt-Jakob disease, BMJ : British Medical Journal, 313: 833-34.

Wopfner, F., G. Weidenhofer, R. Schneider, A. von Brunn, S. Gilch, T. F. Schwarz, T. Werner, and H. M. Schatzl. 1999. Analysis of 27 mammalian and 9 avian PrPs reveals high conservation of flexible regions of the prion protein, J Mol Biol, 289: 1163-78.

Xanthopoulos, K., M. Polymenidou, S. J. Bellworthy, S. L. Benestad, and T. Sklaviadis. 2009. Species and strain glycosylation patterns of PrP^{Sc}, PLoS One, 4: e5633.

국 문 초 록

소 프리온 단백질 유전자 과발현 형질전환 마우스를 이용한 소해면상뇌증 지속감염 세포의 생물학적 및 생화학적 특성 분석

서 태 영

(지도교수 : 김대용)

서울대학교 대학원 수의학과

수의병리학 전공

과거 확립된 정형 소해면상뇌증 (C-BSE)이 지속감염 된 M2B 세포주는 기존의 프리온 질병의 특성 분석에 쓰이는 마우스 바이오어세이법을 대체할 수 있는 수단으로 여겨진다. 이를 위해서는 M2B 세포주와 C-BSE가 동일한 특성을 가지는 지에 대한 분석이 필요하다. 본 실험에서는 M2B 세포주와 C-BSE 감염 소의 뇌유제액을 소의 정상 프리온 단백질을 과발현하도록 디자인된 형질전환 마우스에

뇌내 접종하여, 생물학적 및 생화학적 특성을 분석하였다. 잠복기는 접종 후 M2B 세포주 접종군 451 ± 7일, C-BSE 접종군 465 ± 31일로 나타났으며, 뇌의 조직병리학적 검사인 lesion profiling 검사법을 수행할 결과 두 그룹 모두 dorsal medulla nuclei, central thalamus, septal nuclei, mesencephalic tegmentum에서 높은 공포지수를 나타냈으며, 면역조직화학염색 결과 두 그룹 모두 공포주위에 변형프리온 침착이 관찰되었다. 생화학적 분석을 위해 두 그룹에 구아니딘염산을 0M에서 4M의 농도로 처리하였을 때, 유사한 농도에서 변형프리온이 용해되었으며, 탈당화 이후 유사한 분자량의 변형프리온이 각각 관찰되었다. 위의 생물학적 및 생화학적 특성분석 결과들을 종합했을 때, M2B 세포주에서 유지되고 있는 변형프리온은 소해면상뇌증과 동일한 계통으로 여겨진다.

.....

주요어 : 소해면상뇌증, M2B 세포주, 특성분석, 소해면상뇌증 지속감염 세포주, 마우스바이오어세이

학번 : 2015-21817